European Journal of Pharmacology 882 (2020) 173238

Contents lists available at ScienceDirect

European Journal of Pharmacology

journal homepage: www.elsevier.com/locate/ejphar

Full length article

Role of JAK-STAT signaling in the pathogenic behavior of fibroblast-like synoviocytes in rheumatoid arthritis: Effect of the novel JAK inhibitor peficitinib

Takashi Emori[a,*], Michiko Kasahara[a,d], Shingo Sugahara[a], Motomu Hashimoto[b], Hiromu Ito[c], Shuh Narumiya[d], Yasuyuki Higashi[a], Yasutomo Fujii[a]

[a] Drug Discovery Research, Astellas Pharma Inc., 21 Miyukiga-oka, Tsukuba, Ibaraki, 305-8585, Japan
[b] Department of Advanced Medicine for Rheumatic Diseases, 54 Kawara-cho, Shougo-in, Sakyo-ku, Kyoto, 606-8507, Japan
[c] Department of Orthopedic Surgery, Kyoto University Graduate School of Medicine, 54 Kawara-cho, Shougo-in, Sakyo-ku, Kyoto, 606-8507, Japan
[d] Alliance Laboratory for Advanced Medical Research, Kyoto University Graduate School of Medicine, Kyoto, 606-8507, Japan

ARTICLE INFO

Keywords:
Rheumatoid arthritis
Fibroblast-like synoviocytes
Janus kinase
Signal transducer and activator of transcription
Peficitinib

ABSTRACT

Rheumatoid arthritis (RA) fibroblast-like synoviocytes (RA-FLS) play a crucial role in the pathogenesis of RA. RA-FLS display passive pro-inflammatory responses and self-directed aggressive responses, such as pro-inflammatory mediator production, reduced apoptosis and formation of a thickened synovial lining. Evidence suggests a role for Janus kinase (JAK)-signal transducer and transcriptional activator (STAT) signaling in the passive response but the aggressive behavior of RA-FLS is poorly understood.

The pharmacologic effects of the novel JAK inhibitor, peficitinib, on cytokine-induced intracellular signaling and self-directed aggressive behavior of RA-FLS (e.g., increased expression of apoptosis-resistant genes and sodium nitroprusside-induced apoptosis) were investigated and compared with approved JAK inhibitors. RA-FLS assembly to form a lining-like structure and pro-inflammatory mediator production was investigated in three-dimensional (3D)-micromass culture.

Peficitinib inhibited STAT3 phosphorylation in RA-FLS following induction by interferon (IFN)-α2b, IFN-γ, interleukin (IL)-6, oncostatin M, and leukemia inhibitory factor in a concentration-related manner, and was comparable to approved JAK inhibitors, tofacitinib and baricitinib. Peficitinib and tofacitinib suppressed autocrine phosphorylation of STAT3 and expression of apoptosis-resistant genes, and promoted cell death. In 3D-micromass culture, peficitinib reduced multi-layered RA-FLS cells to a thin monolayer, an effect less pronounced with tofacitinib. Both compounds attenuated production of vascular endothelial growth factor-A, matrix metalloproteinases, IL-6 and tumor necrosis factor superfamily-11.

This study confirmed the pathogenic role of uncontrolled JAK-STAT signaling in the aggressive and passive responses of RA-FLS that are critical for RA progression. The novel JAK inhibitor peficitinib suppressed the pro-inflammatory behavior of RA-FLS, accelerated cell death and abrogated thickening of the synovium.

1. Introduction

Rheumatoid arthritis (RA) is a systemic autoimmune disease characterized by synovial inflammation and joint destruction. Under normal conditions, the cells of the synovial membrane (fibroblast-like synoviocytes; FLS) assure the integrity of joints by controlling the composition of the synovial fluid and extracellular matrix of the joint lining. In RA, chronic inflammation causes phenotypic conversion of FLS to RA-FLS, which proliferate, leading to a thickened synovial membrane, or "pannus", and subsequent joint destruction. RA-FLS produce pro-inflammatory mediators that degrade and remodel the tissue (Bottini and Firestein, 2013; Cho et al., 2002; Lefevre et al., 2015) and tumor necrosis factor (TNF) superfamily-11 (TNFSF11; or receptor activator of nuclear factor κB ligand: RANKL), involved predominantly in bone erosion (Takayanagi et al., 2000).

Biological cytokine inhibitors, such as anti-TNF-α and anti-

* Corresponding author. Drug Discovery Research, Astellas Pharma Inc., 21 Miyukiga-oka, Tsukuba, Ibaraki, 305-8585, Japan.
E-mail addresses: takashi.emori@astellas.com (T. Emori), michiko.kasahara@astellas.com (M. Kasahara), shingo.sugahara@astellas.com (S. Sugahara), mohashim@kuhp.kyoto-u.ac.jp (M. Hashimoto), hiromu@kuhp.kyoto-u.ac.jp (H. Ito), snaru@mfour.med.kyoto-u.ac.jp (S. Narumiya), y.higashi@healios.jp (Y. Higashi), yasutomo.fujii@astellas.com (Y. Fujii).

https://doi.org/10.1016/j.ejphar.2020.173238
Received 21 June 2019; Received in revised form 27 May 2020; Accepted 29 May 2020
Available online 16 June 2020

interleukin (IL)-6 receptor antibodies, have revolutionized the management of RA over the past two decades (Wang et al., 2014). However, RA pathogenesis is multifactorial and complex, and optimization of management requires broader control of inflammatory cytokines and processes. Another approach to RA therapy would be to target the aggressive behavior of RA-FLS, such as increased survival, adhesion and invasiveness, and lining cell condensation to produce the thickened, hyperplastic pannus (Bottini and Firestein, 2013; Kiener et al., 2006). Notably, upregulation of apoptosis-resistant genes drives the development of hyperplasia (Bartok and Firestein, 2010).

The Janus kinase (JAK) family (JAK1, JAK2, JAK3 and tyrosine kinase-2: TYK2) of non-receptor tyrosine kinases plays a crucial role in cytokine signaling implicated in the pathogenesis of RA. Activated JAKs recruit signal transducer and activator of transcription (STAT) proteins (STAT1, 2, 3, 4, 5A, 5B and 6), which translocate to the nucleus and activate their target genes. Currently, more than 40 different cytokines and growth factors have been shown to activate specific combinations of JAKs and STATs (Nakayamada et al., 2016). STAT3 may be important for RA pathogenesis, particularly in synovitis, although the specific role of STAT proteins remains to be clarified (Gao et al., 2015).

A number of JAK inhibitors have been marketed as new therapies for RA (Nakayamada et al., 2016). Tofacitinib inhibits JAK1, JAK2, JAK3 and to a lesser extent TYK2. Baricitinib inhibits JAK1 and JAK2 with better selectivity than JAK3 (Nakayamada et al., 2016). Peficitinib is a novel pan-JAK inhibitor that inhibits JAK1, JAK2, JAK3 and TYK2 (Ito et al., 2017). The efficacy and safety profile of these compounds in clinical trials highlight the critical role of JAK-STAT pathways in the pathogenesis of RA and emphasize the potential for JAK inhibitors to provide alternative therapies in the treatment of RA (Nakayamada et al., 2016). While there is clear evidence of a role for JAK-STAT signaling in the cytokine response and migration of RA-FLS (Diller et al., 2019; Ikari et al., 2019), the role of the pathway in the self-directed aggressive behavior of RA-FLS is poorly understood.

The present study investigates the pharmacologic profile of peficitinib on JAK-STAT signaling in RA-FLS and its effect on sodium nitroprusside-induced apoptosis. Using a three-dimensional (3D) culture system that recapitulates the diseased phenotypes in RA-FLS, we further investigated the effect of peficitinib on the spontaneous production of pro-inflammatory mediators and formation of a thickened lining-like cell structure.

2. Materials and methods

2.1. Study approval

In this study, no animal experimentation occurred, with no animal ethics committee required. Ethical approval for experiments with human samples in this study was granted by the Ethics Committee of Kyoto University Graduate School and the Faculty of Medicine (approval number: G418), and Astellas Research Ethics Committee (approval number: 120182). Informed consent was obtained from all patients prior to sample collection.

2.2. Patient-derived FLS

RA and osteoarthritis (OA) were diagnosed according to the criteria of the American College of Rheumatology (Altman et al., 1986; Arnett et al., 1988). Synovial tissues were obtained from patients with OA and RA undergoing orthopedic surgery. RA-FLS were isolated from synovial tissue as described previously (Emori et al., 2017) and maintained in Dulbecco's modified Eagle's medium (Gibco, Paisley, UK) supplemented with 10% heat-inactivated fetal bovine serum (FBS) (Hyclone from GE Healthcare, Buckinghamshire, UK or FBS from Biosera, Kansas City, MO), 100 units/ml of penicillin, and 100 μg/ml of streptomycin sulfate (Nacalai Tesque, Kyoto, Japan) in an incubator at 5% CO_2 at 37 °C. FLS that had been passaged 4–10 times after the start of the culture were used as isolated FLS.

2.3. Test reagents

Peficitinib, tofacitinib and baricitinib were synthesized in Astellas Pharma Inc., and were stocked as 10 mM dimethyl sulfoxide (DMSO) solution. The compounds were diluted in culture medium supplemented with 1% DMSO at ten times the desired concentration and added to the wells of a 96-well plate at one-tenth of the final volume. IL-6 receptor-blocking antibody (MAB227) and isotype-matched control antibody (MAB002) were purchased from R&D Systems (Minneapolis, MN) and diluted in culture medium.

2.4. Immunofluorescent staining

Immunofluorescent staining was performed as described previously (Emori et al., 2017). Acquisition of microscopy images was performed by NIS-Elements (version 3.2, Nikon Corporation, Tokyo, Japan). The primary and secondary antibodies used in this study were as follows: rabbit immunoglobulin (Ig)G isotype control (clone DA1E, Cell Signaling Technology, Danvers, MA), anti-phosphorylated STAT3 (rabbit monoclonal antibody, clone EP2147Y, Abcam, Cambridge, UK), anti-phosphorylated STAT1 (rabbit monoclonal antibody, clone 58D6, Cell Signaling Technology), anti-phosphorylated STAT4 (rabbit monoclonal antibody, clone D2E4, Cell Signaling Technology), anti-phosphorylated STAT5 (rabbit monoclonal antibody, clone C71E5, Cell Signaling Technology), Alexa flour 488-conjugated anti-rabbit IgG (Life Technologies, Carlsbad, CA). DAPI (4′,6-diamidino-2-phenylindole, Nacalai Tesque, Kyoto, Japan) was added at 1 μg/ml to the secondary antibody solution.

2.5. Cell-based enzyme-linked immunosorbent assay (ELISA)

RA-FLS (2×10^4 cells) were seeded in 96-well plates and incubated in a CO_2 incubator. The following day, the culture supernatants were exchanged with fresh medium (40 μl). After addition of 10 μl of a 10 × solution of test compounds or test antibodies, the plates were further incubated for 20 min. Ligand stimulation was performed by adding twice the concentration of the indicated ligands (50 μl) and incubating for 20 min. The cells were then fixed in phosphate buffered saline (PBS)-buffered 8% formaldehyde (100 μl) for 10–20 min, washed with PBS and permeabilized by incubation in ice-cold methanol (100 μl) for 10 min. After washing with PBS extensively, the cells were blocked with PBS-buffered 1% bovine serum albumin (BSA) (150 μl) for 1 h and stained with anti-phosphorylated STAT3 (rabbit monoclonal antibody; EP2147Y; Abcam), diluted 1:500 in PBS-buffered 1% BSA (50 μl), for 2 h. The cells were washed with PBS and further incubated with horseradish peroxidase (HRP)-linked anti-rabbit IgG (Cell signaling technology), diluted 1:2000 in PBS-buffered 1% BSA, for 1 h. The signal was developed using 1-Step Ultra 3,3′,5,5′-tetramethylbenzidine-ELISA (50 μl, Thermo Fisher Scientific, Waltham, MA) and measured using a microplate reader after addition of 4N sulfuric acid (50 μl, Nacalai Tesque, Kyoto Japan). The recombinant human cytokines were purchased and used as indicated: interferon (IFN)-α2b (1000 ng/ml, BioVision, Milpitas, CA), IFN-γ (100 ng/ml, R&D Systems), IL-6 (200 ng/ml, R&D Systems), IL-15 (100 ng/ml, R&D Systems), IL-21 (100 ng/ml, PeproTech, Rocky Hill, NJ), TNF-α (100 ng/ml, R&D Systems), leukemia inhibitory factor (LIF) (100 ng/ml, R&D Systems), oncostatin M (OSM) (100 ng/ml, R&D Systems), sIL-6 receptor (200 ng/ml, PeproTech).

2.6. Determination of phosphorylated STAT3 and total STAT3 protein levels

Test compounds were diluted 1:10 in medium supplemented with 1% DMSO and dispensed into 6-well plates (0.2 ml/well), and OA- or

RA-FLS cell suspensions were added (2.8–6.0 × 10^4 cells/ml, 1.8 ml/well). For the control well, 1.8 ml of cell suspension was added with 0.2 ml of medium supplemented with 1% DMSO. The cells were grown in a CO_2 incubator for 6 days to reach confluence. Cellular phosphorylated (p)STAT3 and total STAT3 levels were examined in cell lysates prepared from the cells (23 μg) using a STAT3 (pY705) plus total STAT3 ELISA Kit (Abcam) and determined from the absorbance at 450 nm according to the manufacturer's instructions. Because the kit was designed as a semi-quantitative measurement method that did not utilize standard curves, the absorbance values were compared using statistical analyses.

2.7. Gene expression analysis

Total RNA was extracted from cells using an RNeasy plus mini RNA extraction kit (Qiagen, Hilden, Germany). Complementary DNA was synthesized from 50 ng of RNA using the SuperScript IV first-strand synthesis system (Thermo Fisher Scientific) and subjected to real-time polymerase chain reaction (PCR) in a Quadro studio real-time PCR system (Applied Biosystems, Foster City, CA) using TaqMan gene expression master mix (Applied Biosystems). The following TaqMan primers were purchased from Applied Biosystems and used in real-time PCR: BCL2 (Hs00608023_m1), MCL1 (Hs01050896_m1), GAPDH (Hs02786624_g1). Gene expression levels were also determined by microarray analysis using SurePrint G3 Human GE 8 × 60K v2 Microarray (Agilent technologies, Santa Clara, CA) with total RNA prepared using the procedure described above and analyzed by GeneSpring GX (Agilent technologies).

2.8. Apoptosis assay

OA- and RA-FLS (2 × 10^4 cells) were seeded in 96-well plates and cultured overnight. The culture medium was replaced with fresh medium (80 μl) and 10 × solutions of inhibitors or 1% DMSO (10 μl; control) and 20 mM of sodium nitroprusside (10 μl) (Sigma-Aldrich, St Louis, MO) were added to the wells. The plates were incubated for 5 h in a CO_2 incubator. The rate of apoptosis was determined by measuring the remaining viable cells in the 3-(4,5-dimethylthiazol-2-yl)-2,5-diphenyltetrazolium bromide (MTT) assay using the CellTiter-96 non-radioactive cell proliferation assay (Promega, Madison, WI).

2.9. 3D-micromass culture and quantification of the lining-like structure

Compounds and blocking antibodies in the 3D-micromass culture were examined as previously described (Emori et al., 2017) with a slight modification. To activate IL-6-mediated signaling, recombinant sIL-6 receptor (PeproTech) was added to the culture medium (50 ng/ml) during the last two weeks of incubation. Thickness of the lining-like structure was measured using image analysis of phalloidin-stained sections of the 3D-micromass architecture as described previously (Emori et al., 2017).

2.10. Western blotting

Preparation of cell lysates from 3D-cultured FLS and subsequent western blotting analyses were performed as described previously (Emori et al., 2017). The antibodies used in the experiments were as follows: anti-pSTAT3 (rabbit monoclonal antibody; EP2147Y; Abcam), anti-human STAT3 (rabbit monoclonal antibody; D1B2J; Cell Signaling Technology), anti-human integrin α9 (rabbit monoclonal antibody; EPR9722; Abcam), anti-human cadherin-11 (rabbit polyclonal antibody; LS-B2308; LSBio, Seattle, WA), anti-human TNFSF11 (goat polyclonal antibody; AF626; R&D Systems), anti-human GAPDH (mouse monoclonal antibody; 6C5; Santacruz Biotechnology, Dallas, TX), HRP-conjugated anti-mouse IgG (NA931V; GE Healthcare) and HRP-conjugated anti-rabbit IgG (NA934V; GE Healthcare).

2.11. ELISA for secreted proteins

The amount of secreted protein in culture supernatants was determined by ELISA using the following commercially available kits: matrix metalloproteinase (MMP)-1 (human total MMP-1 DuoSet ELISA; R&D Systems), MMP-3 (human total MMP-3 DuoSet ELISA; R&D Systems), IL-6 (human IL-6 DuoSet ELISA; R&D Systems), vascular endothelial growth factor-A (VEGF-A, human VEGF-A ELISA kit; RayBiotech, Norcross, GA). Half of the detection limit value indicated in the instruction was adopted when the sample value was below the lower limit of quantification.

2.12. Statistical analysis

Statistical analyses and calculation of IC_{50} values were performed using GraphPad Prism 7 software (GraphPad Software, La Jolla, CA). A P value < 0.05 was considered statistically significant.

3. Results

3.1. Phosphorylation of STAT3 is enhanced in RA synovial tissue

To determine the JAK-STAT pathways activated in RA synovial tissues, we conducted immunofluorescent staining of frozen RA tissue sections using antibodies against pSTAT1, pSTAT3, pSTAT4 and pSTAT5 in combination with DAPI. Staining was also performed on OA tissue sections for comparison. pSTAT3-positive cells were widely and abundantly distributed across the hyperplastic region in RA tissue but were rare in OA tissue (Fig. 1A). In addition, pSTAT3 staining overlapped with DAPI staining in RA tissue, indicating nuclear localization (Fig. 1B). Further immunofluorescence analysis is needed to investigate whether the unphosphorylated STAT3 level is also increased in RA tissue compared with OA tissue. In contrast, there was no apparent pSTAT1, pSTAT4 or pSTAT5 staining in either RA or OA tissue (data not shown). These results indicate that STAT3 is activated in RA synovium, suggesting a role for STAT3 in the pathogenesis of RA.

3.2. JAK inhibitors block STAT3 phosphorylation induced by various cytokines in RA-FLS

To identify the cytokines that induce pSTAT3 in RA tissue, we examined the ability of various cytokines to induce STAT3 phosphorylation in RA-FLS isolated from RA tissue. RA-FLS were stimulated with various cytokines and the level of pSTAT3 determined. Phosphorylation of STAT3 was markedly induced following stimulation with IFN-α2b (1000 ng/ml), IFN-γ (100 ng/ml), LIF (100 ng/ml) and OSM (100 ng/L), but not TNF-α (100 ng/ml), IL-15 (100 ng/ml) and IL-21 (100 ng/ml) (Fig. 2A). Stimulation with IL-6 (200 ng/ml) also increased levels of pSTAT3, and addition of sIL-6 receptor (200 ng/ml) further increased these levels (Fig. 2A). These results indicate that IFN-α2b, IFN-γ, OSM, LIF, IL-6 and sIL-6 receptor may contribute to the constitutive phosphorylation of STAT3 in RA tissue.

We subsequently compared the effect of peficitinib with tofacitinib and baricitinib on the induction of pSTAT3 by IFN-α2b, IFN-γ, LIF and OSM in RA-FLS using cell-based ELISA. RA-FLS were treated with various concentrations of JAK inhibitors, stimulated with cytokines and subjected to cell-based ELISA to determine the levels of pSTAT3. All the JAK inhibitors blocked the induction of pSTAT3 by the cytokines tested in a similar concentration-related manner (Fig. 2B). Although their 50% inhibition concentration (IC_{50}) values differed slightly, the significance of this difference was unclear because of wide 95% confidence intervals (Table 1).

The IC_{50} values were calculated by non-linear curve fitting in the assays described in Fig. 2B. The geometric mean of the IC_{50} values from four independent experiments is shown with 95% confident intervals. The specific JAK family members associated with the indicated

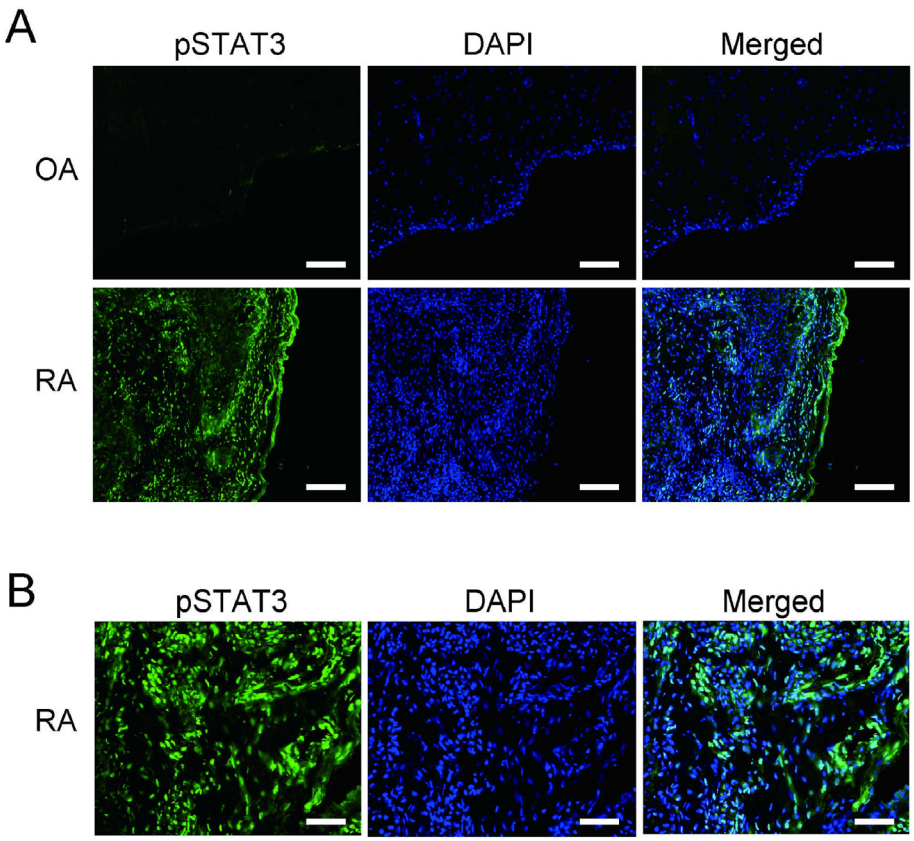

Fig. 1. Constitutive activation of STAT3 in RA synovial tissue. (A) Fluorescent micrographs of phosphorylated STAT3 protein in RA and OA synovial tissue. Frozen sections from OA (upper) and RA tissue (lower) were stained with an antibody against pSTAT3 and Alexa Fluor 488-labeled secondary antibody and counterstained with DAPI. The sections were photographed under a fluorescent microscope at the same exposure time. Representative images of tissues from three independent patients are shown. Scale bars: 200 μm. (B) High magnification images of the RA tissues in (A). Scale bars: 100 μm.

cytokine receptors are shown according to previous reports (Banerjee et al., 2017; Heinrich et al., 1998).

IC_{50}, half maximal inhibitory concentration; IFN, interferon; IL-6, interleukin-6; JAK, Janus kinase; LIF, leukemia inhibitory factor; OSM, oncostatin M; sIL-6, soluble interleukin-6.

3.3. JAK inhibitors suppress enhanced phosphorylation of STAT3 and promote apoptosis of RA-FLS

We next examined whether JAK activation is involved in the enhanced phosphorylation of STAT3. OA- and RA-FLS were grown to confluence in medium supplemented with or without peficitinib or tofacitinib at the various concentrations, and pSTAT3 and total STAT3 protein levels in lysates prepared from the cells were then determined using ELISA. Phosphorylated STAT3 and total STAT3 protein levels in RA-FLS were significantly higher than those in OA-FLS, and treatment of RA-FLS with peficitinib and tofacitinib decreased the elevated levels of pSTAT3, indicating that enhanced phosphorylation of STAT3 in RA-FLS is JAK dependent (Fig. 3A). In addition, peficitinib, but not tofacitinib, tended to reduce total STAT3 protein levels at 1000 nM (Fig. 3A).

Activation of STAT3 imparts anti-apoptotic ability to RA-FLS through upregulation of the B-cell leukemia/lymphoma 2 protein (BCL2) family of anti-apoptotic genes (Lee et al., 2013; Zhao et al., 2017). Therefore, we determined gene expression levels of BCL2 and myeloid cell leukemia sequence 1 (MCL1) using real-time PCR with RNA prepared from the above cells. Compared with OA-FLS, RA-FLS displayed increased expression of these anti-apoptotic genes, and treatment with peficitinib and tofacitinib attenuated this increase, indicating that RA-FLS employ increased expression of anti-apoptotic genes in a JAK-dependent manner, and that autonomous activation of the JAK-STAT pathway is responsible for the enhanced expression of anti-apoptotic genes in RA-FLS (Fig. 3B). We also determined whether treatment with JAK inhibitors promotes cell death in RA-FLS via sodium nitroprusside, which generates nitric oxide to induce apoptosis (Xie et al., 1997). RA-FLS grown in 96-well plates were treated with the JAK inhibitors in combination with soluble nitroprusside for 5 h. The degree of cell death was calculated according to viability in the MTT assay (Fig. 3C). Treatment of RA-FLS with the JAK inhibitors themselves did not cause apparent cell death (Fig. 3C, white bars). However, addition of 2 mM soluble nitroprusside to DMSO-treated RA-FLS caused a 38.4% increase in cell death compared to the DMSO only control. Cell death increased by 63.8% and 52.8% when soluble nitroprusside was combined with peficitinib and tofacitinib, respectively, compared to the control treated with the respective JAK inhibitors alone (Fig. 3C, black bars). These results indicate that JAK inhibitors can accelerate soluble nitroprusside-induced apoptosis in RA-FLS.

3.4. JAK inhibitors prevent formation of a hyperplastic lining-like structure by RA-FLS grown in 3D-micromass culture

Given that the anti-apoptotic ability of RA-FLS is considered one of the drivers of synovial lining hyperplasia in RA, we examined the action of JAK inhibitors on the formation of the hyperplastic lining-like structure using a previously described 3D-micromass culture system (Emori et al., 2017). Isolated RA-FLS were embedded in Matrigel and cultured in 3D-micromass for 3 weeks with various concentrations of peficitinib or tofacitinib. To promote the response of RA-FLS to autonomously produced IL-6, sIL-6 receptor was added to the culture during the last 2 weeks. The resultant architectures were freeze-fixed, sectioned and stained with fluorescent-labeled phalloidin to visualize the lining-like structure. Control RA-FLS grown in the 3D-culture autonomously formed multi-layered lining-like cell condensation (Fig. 4), a structure that was abrogated and reduced to almost a thin monolayered lining following treatment with peficitinib (Fig. 4). Subsequent quantitative analysis of the microscopic images revealed that treatment with peficitinib caused a concentration-related reduction in the thickness of the lining-like structure (up to 78.0% of the DMSO control;

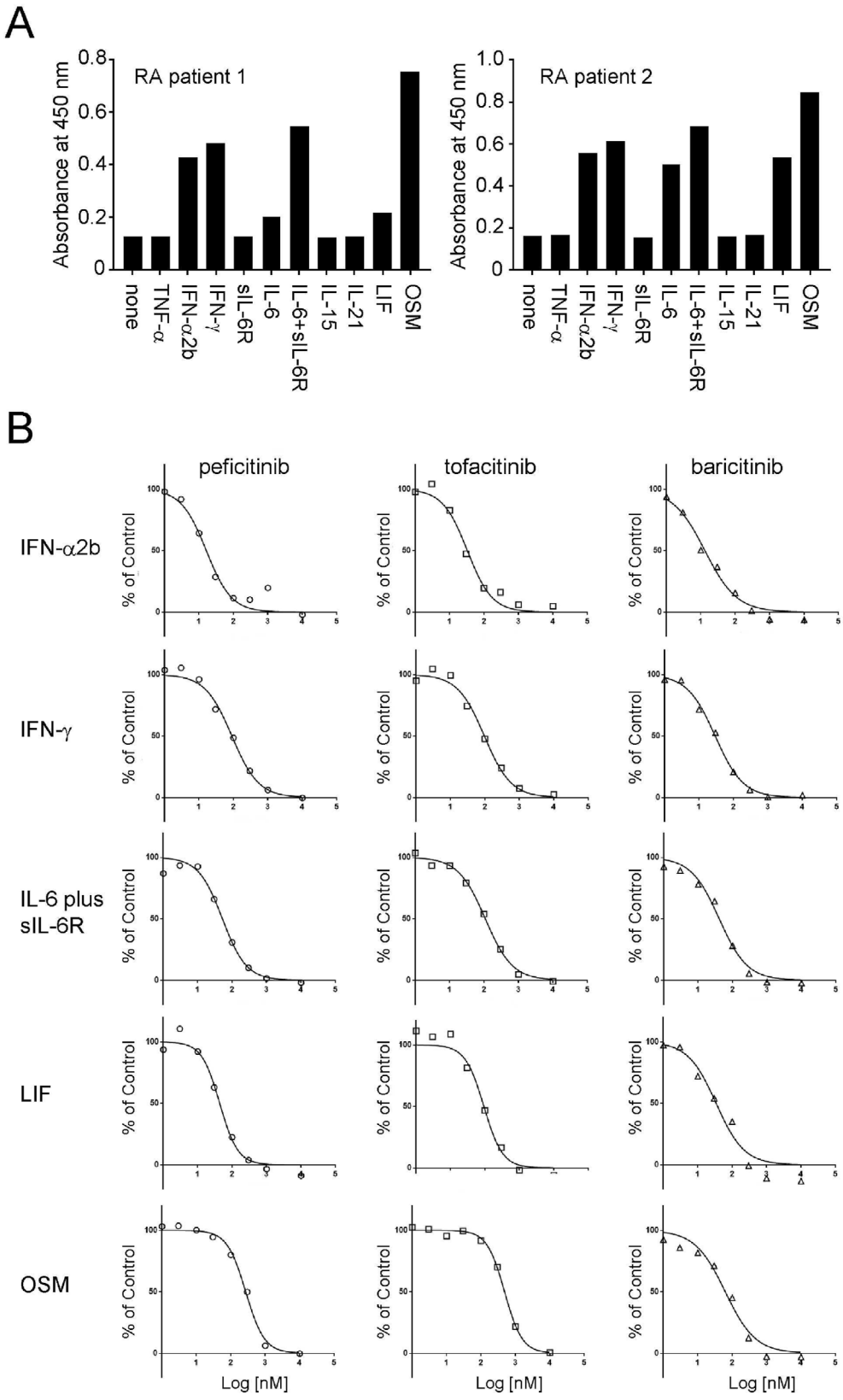

Fig. 2. Inhibitory profile of peficitinib, tofacitinib and baricitinib against pSTAT3 induction by various cytokines in RA-FLS. (A) Induction of pSTAT3 in RA-FLS by various cytokines. RA-FLS, cultured in 96-well plates, were stimulated with the indicated cytokines and subjected to cell-based ELISA to determine pSTAT3 levels. Data represent the mean value of triplicate assays. Patient 1 and 2 indicate assays using RA-FLS from independent patients. (B) Inhibitory profile of peficitinib, tofacitinib and baricitinib against pSTAT3 induction by various cytokines. RA-FLS were stimulated with the indicated cytokines with or without peficitinib, tofacitinib or baricitinib. pSTAT3 levels were determined using cell-based ELISA and expressed as a percentage of the DMSO control. IC_{50} values of each compound were calculated using non-linear curve fitting and are summarized in Table 1. The experiments were performed using RA-FLS from three to five patients and representative fitted curves are shown. Each plot indicates the mean value of duplicate assays. Open circle: peficitinib, open square: tofacitinib, open triangle: baricitinib. IFN, interferon; IL, interleukin; JAK, Janus kinase; LIF, leukemia inhibitory factor; OSM, oncostatin M; sIL, soluble interleukin; TNF, tumor necrosis factor.

Fig. 4). Although not significant, tofacitinib displayed a clear trend towards decreasing the thickness of the lining-like structure (up to 88.8% of the DMSO control; Fig. 4).

We also determined the pSTAT3 levels in the cells grown in the 3D-micromass culture. Cell lysates prepared from the architectures were subjected to western blotting using an antibody against pSTAT3 followed by reprobing with an antibody against total STAT3 and GAPDH. The marked phosphorylation of STAT3 observed in the DMSO control was decreased by a similar extent following treatment with peficitinib and tofacitinib (Fig. 4). The decrease of total STAT3 protein observed

Table 1
JAK inhibitor IC_{50} values for inhibition of cytokine-stimulated pSTAT3 induction in RA-FLS.

Ligand/cytokine	Associated JAK	IC_{50} (nM) [95% confidence interval] (n)		
		Peficitinib	Tofacitinib	Baricitinib
IFN-α2b	JAK1, TYK2	11.95 [7.35 to 19.42] (n = 4)	19.47 [7.08 to 53.54] (n = 4)	7.59 [3.32 to 17.32] (n = 4)
IFN-γ	JAK1, JAK2	62.27 [25.04 to 154.9] (n = 4)	75.82 [46.7 to 123.1] (n = 4)	23.73 [16.22 to 34.72] (n = 4)
IL-6 plus sIL-6 receptor	JAK1, JAK2, TYK2	81.68 [51.53 to 129.5] (n = 5)	164.3 [113.4 to 238.0] (n = 5)	27.04 [14.71 to 49.7] (n = 4)
OSM	JAK1, JAK2, TYK2	149.1 [84.85 to 262.1] (n = 5)	302.8 [199.1 to 460.5] (n = 5)	69.8 [58.38 to 83.46] (n = 4)
LIF	JAK1, JAK2, TYK2	31.03 [14.43 to 66.71] (n = 4)	83.3 [68.18 to 101.8] (n = 4)	36.41 [28.05 to 47.25] (n = 3)

following treatment with peficitinib in plate-cultured RA-FLS (Fig. 3A) was also observed in the cells grown in the 3D-micromass culture (Fig. 4). Subsequently, we investigated the effect of an IL-6 receptor antibody in the same 3D-culture assay. Like peficitinib, IL-6 receptor antibody blocked pSTAT3 induction by IL-6 plus sIL-6 receptor in RA-FLS using cell-based ELISA (Fig. 4) but, in contrast to the effect observed for JAK inhibitors, there was no apparent reduction in the lining thickness following treatment of the architectures with the IL-6 receptor

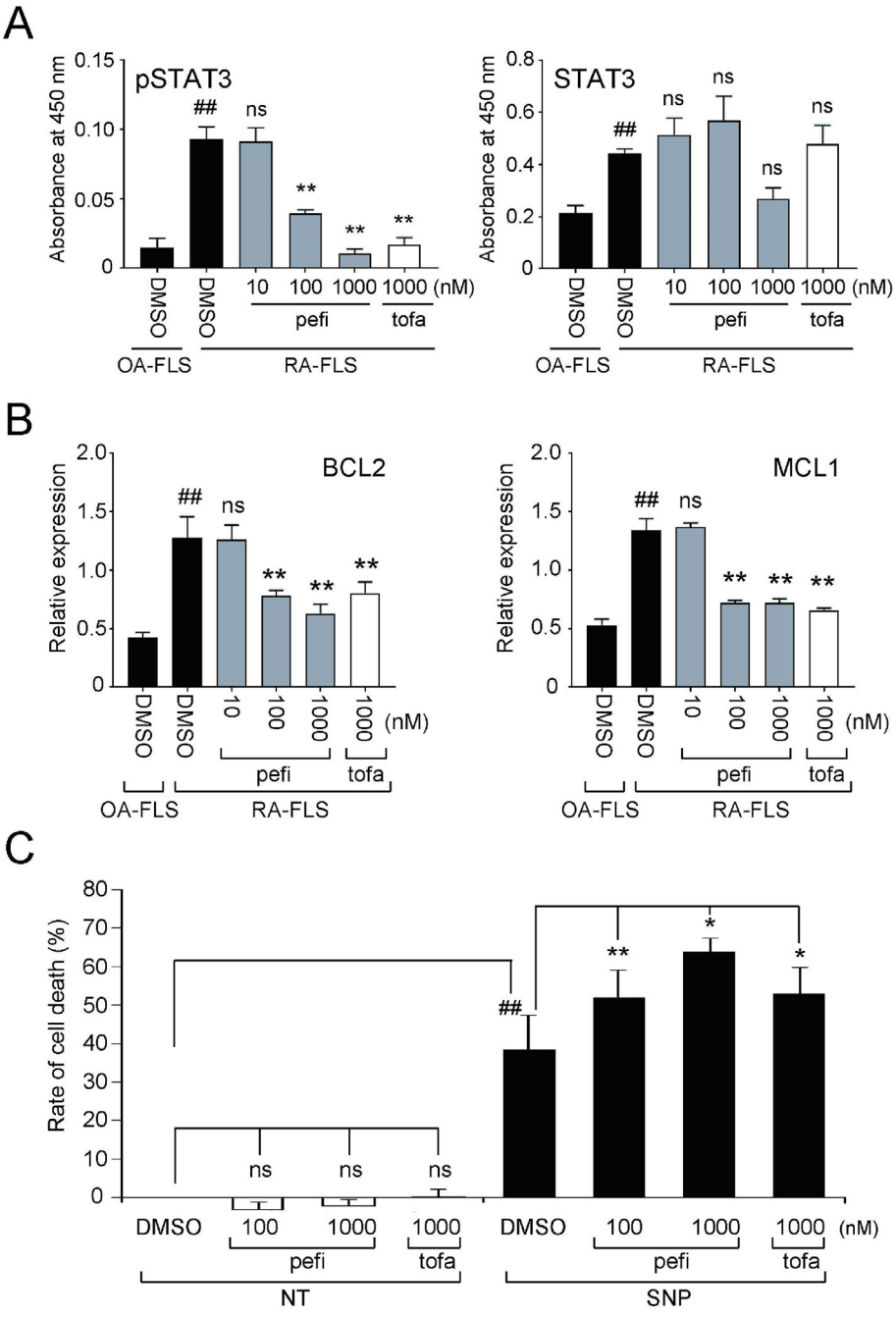

Fig. 3. Effect of JAK inhibitors on increased levels of pSTAT3 and soluble nitroprusside-induced apoptosis induced in RA-FLS. (A and B) Effect of JAK inhibitors on increased levels of pSTAT3 and anti-apoptotic gene expression normalized to that of GAPDH in RA/OA-FLS. Data are expressed as the mean and S.E.M. Statistical analyses were performed using Student's t-test (OA-FLS with DMSO vs RA-FLS with DMSO) and Dunnett's test using within subject error (RA-FLS with DMSO vs RA-FLS with compounds at the indicated concentrations). $^{**/\#\#}P < 0.01$; ns, not significant. (C) Effect of JAK inhibitors on cell death of RA-FLS induced by soluble nitroprusside. Data are expressed as the mean percentage of the non-treated DMSO control and S.E.M. Statistical analyses were performed using a Student's t-test (non-treated control with DMSO vs apoptosis-induced RA-FLS with DMSO) and Dunnett's test using within subject error (RA-FLS with DMSO vs RA-FLS with compounds at the indicated concentrations). $^{*}P < 0.05$; $^{**/\#\#}P < 0.01$; ns, not significant. (A) n = 4; (B) n = 4; (C) n = 6. BCL, B-cell leukemia; FLS, fibroblast-like synoviocytes; MCL, myeloid cell leukemia; OA, osteoarthritis; pefi, peficitinib; pSTAT, phosphorylated signal transducer and transcriptional activator; RA, rheumatoid arthritis; SNP, sodium nitroprusside; tofa, tofacitinib.

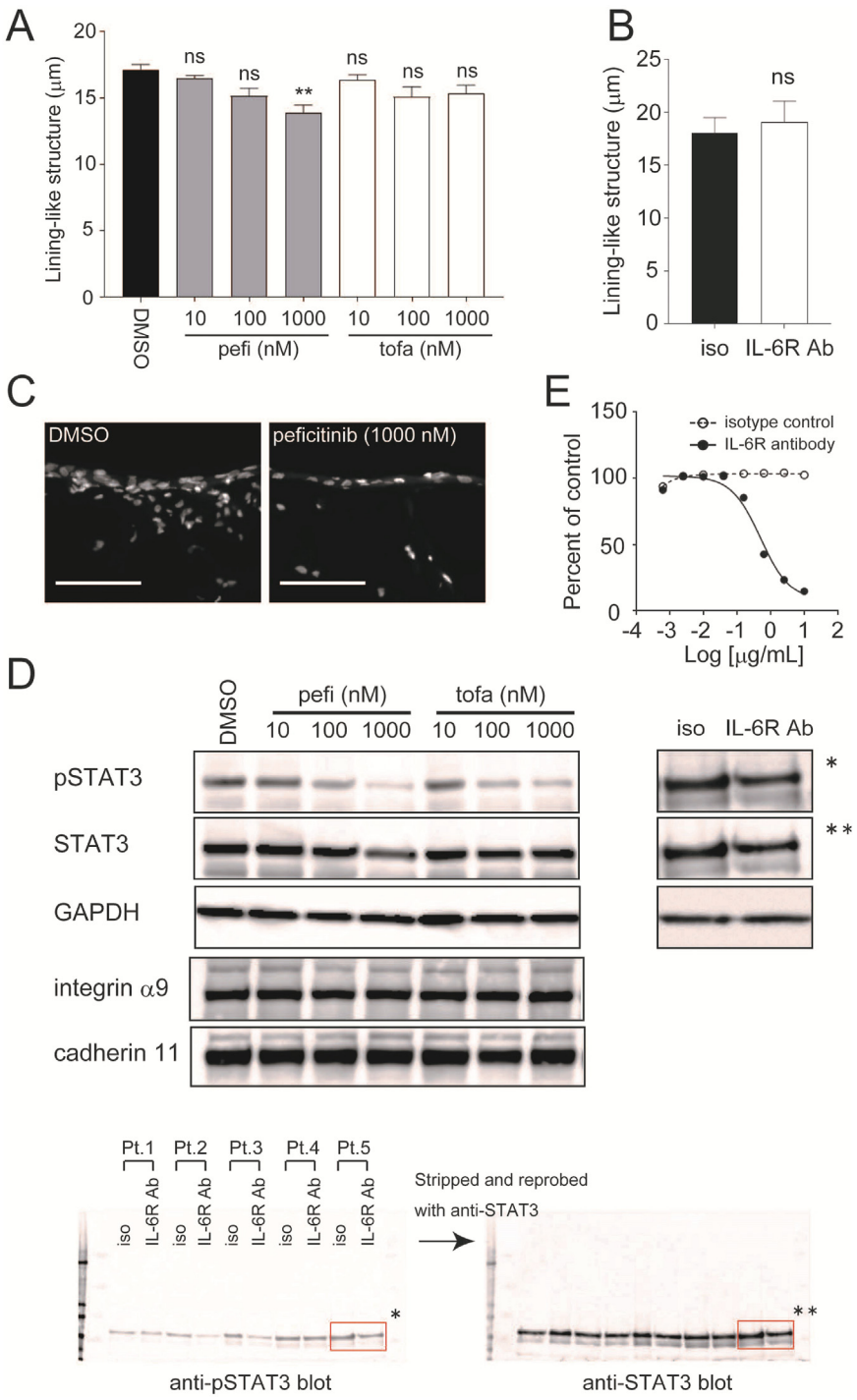

Fig. 4. Effect of JAK inhibitors on self-directed lining-like cell condensation of RA-FLS in 3D-micromass culture. RA-FLS were pretreated with peficitinib (pefi) or tofacitinib (tofa) at the indicated concentrations (A) or 10 μg/ml of interleukin-6R antibody (IL-6 receptor Ab) (B) and maintained in 3D-micromass culture with medium containing the corresponding reagents. An equal amount of DMSO or isotype-matched control antibody (iso) was added to the control. (A and B) The thickness of the lining-like structure of the resultant architectures was calculated using image analyses and expressed as the mean and S.E.M. Statistical analyses were performed using a Dunnett's test using within subject error (A) and paired *t*-test (B). **P < 0.01; ns, not significant. (A) n = 5; (B) n = 5. (C) Typical images of the lining-like structure formed by RA-FLS following treatment with DMSO (left) or peficitinib (1000 nM, right) with DAPI staining. Scale bar: 50 μm. (D) Western blotting of the lysates from the resultant architectures was performed using antibodies against the indicated molecules. Representative data from RA-FLS from three to five independent patients are shown. Lower panel indicates original gel blots of asterisked (*/**) images in upper panel. Pt.1-Pt.5 indicates patient ID. Bands indicated by boxes were cropped and used in the upper panel. (E) Inhibition of pSTAT3 induction by IL-6 plus sIL-6 receptor using an IL-6 receptor antibody in RA-FLS was analyzed using cell-based ELISA and the values were converted to a percentage of the control value from non-treated cells. Data represent the mean of triplicate assays. Closed circle: IL-6 receptor antibody, open circles: isotype-matched control. Non-linear fitted curves for the IL-6 receptor antibody and isotype-matched control are shown as solid and dashed lines, respectively. pSTAT, phosphorylated signal transducer and transcriptional activator.

antibody (Fig. 4). In addition, treatment of 3D-cultured RA-FLS with the IL-6 receptor antibody had no effect on the pSTAT3 or STAT3 protein levels (Fig. 4).

Because integrin α9 and cadherin-11 reportedly mediate aggressive cell condensation into the lining-like structure observed in this system (Emori et al., 2017; Kiener et al., 2006), we also determined the effect of JAK inhibitors on integrin α9 and cadherin-11 protein levels. However, JAK inhibitors had no effect on integrin α9 or cadherin-11 protein levels (Fig. 4), indicating that the effect of JAK inhibitors on the assembly of lining cell condensation is independent of integrin α9 and cadherin-11.

3.5. JAK inhibitors ameliorate the production of pro-inflammatory mediators by RA-FLS grown in 3D-micromass culture

We examined the effect of JAK inhibitors and the IL-6 receptor antibody on the production of pro-inflammatory mediators by RA-FLS cultured in 3D-micromass. To do this, we determined the concentrations of MMP-1, MMP-3, IL-6 and VEGF-A in the supernatants of the 3D-micromass culture performed as described in Materials and Methods. While there was a significant decrease in these mediators in the cell supernatants following treatment with JAK inhibitors, particularly peficitinib (Fig. 5A; tofacitinib did not significantly reduce VEGF-A), there was no such reduction following treatment with the IL-6 receptor antibody (Fig. 5B). In addition, western blotting of the lysates from the

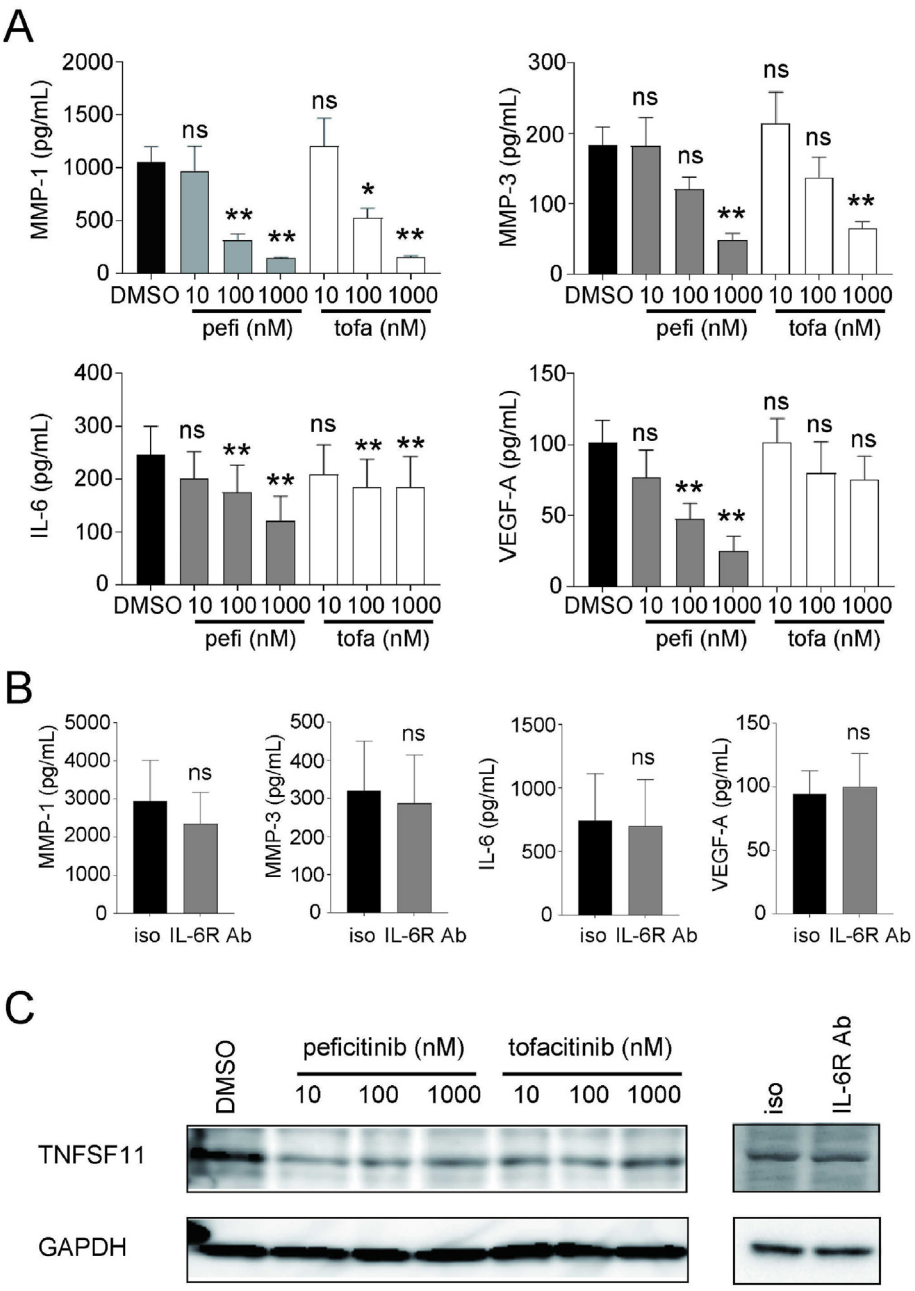

Fig. 5. Effect of JAK inhibitors on autonomous expression of pro-inflammatory mediators in RA-FLS in 3D-micromass culture. (A and B) The supernatants of RA-FLS cultured in 3D-micromass were obtained at the end of the experiments described in Fig. 4 and were analyzed using ELISA for the indicated mediators. Data represent the mean and S.E.M. (A) n = 5; (B) n = 5. Statistical analyses were performed using a Dunnett's test using within subject error (A) and paired *t*-test (B). *P < 0.05; **P < 0.01; ns, not significant. (C) The cell lysates of the micromass architectures prepared in Fig. 4 were analyzed by western blotting using antibodies against the indicated proteins. IL, interleukin; iso, isotype-matched control; MMP, matrix metalloproteinase; pefi, peficitinib; TNFSF11, tumor necrosis factor superfamily-11; tofa, tofacitinib; VEGF, vascular endothelial growth factor.

3D-cultured cells showed that treatment with JAK inhibitors decreased TNFSF11/RANKL protein levels, which were not altered by treatment with the IL-6 receptor antibody (Fig. 5C). These results indicate that JAK inhibitors suppress activation of STAT3, ameliorate the assembly of hyperplastic lining cell condensation and inhibit production of pro-inflammatory mediators in RA-FLS, which cannot be achieved by specific blockade of IL-6 receptor.

3.6. Cytokines and growth factors possibly contribute to formation of hyperplastic lining-like structure associated with RA-FLS

To explore the possible factors involved in the formation of hyperplastic lining-like structure, we determined gene expression levels of various cytokines and growth factors known to induce STAT3 phosphorylation in RA- and OA-FLS grown in 3D-micromass. As a result, although not significant, RA-FLS displayed more abundant expression of IL-6, LIF, OSM, platelet-derived growth factor (PDGF) A, PDGFC and PDGFD than did OA-FLS. This suggests that upregulation of these factors possibly contributes to the formation of hyperplastic lining-like structure in an autocrine manner in RA-FLS (Fig. 6).

4. Discussion

The JAK-STAT pathway is the major mechanism mediating cytokine signaling and cellular response to extracellular stimuli. While the primary action of JAK inhibitors on RA-FLS may be to regulate their passive response to pro-inflammatory cytokines, we hypothesized that the aggressive behavior of RA-FLS may also be associated with excessive activation of JAK-STAT signaling and thus a target for JAK inhibition. We investigated this by determining the effect of JAK inhibitors on the disease-associated phenotypes of RA-FLS.

We found that phosphorylation of STAT3 was enhanced in RA tissue (Fig. 1). Interestingly, RA-FLS retained high STAT3 phosphorylation after isolation from the synovial environment. In addition, the phosphorylation of STAT3 was suppressed by JAK inhibitors (Figs. 3A and 4D). These results suggest that enhanced basal STAT3 activity is one of

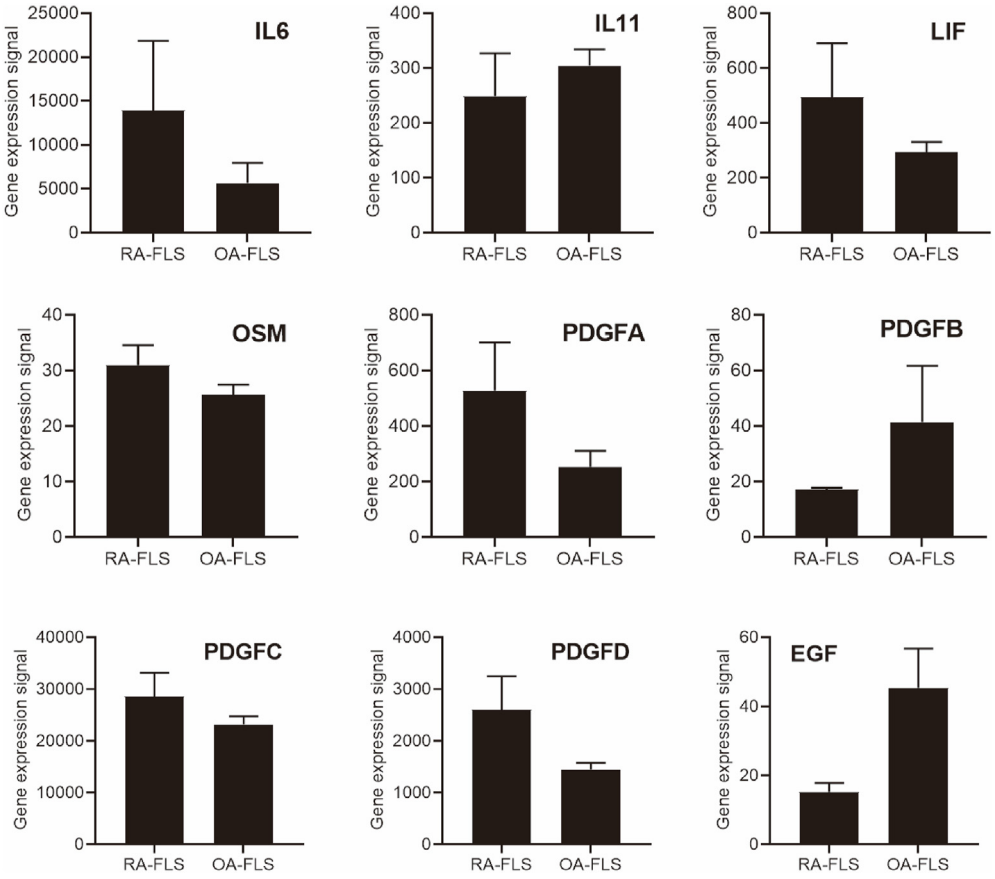

Fig. 6. Gene expression levels of pSTAT3-inducing cytokines and growth factors in RA- and OA-FLS. Total RNA from 3D-cultured RA- and OA-FLS analyzed by microarray and expression levels of the indicated genes are shown. Data represent the mean and S.E.M. (n = 3)
EGF, epidermal growth factor; IL, interleukin; LIF, leukemia inhibitory factor; OSM, oncostatin M; PDGF, platelet-derived growth factor.

the abnormal properties of RA-FLS, and is induced by JAK-mediated cytokine signaling.

Platelet-derived growth factor and epidermal growth factor are reportedly involved in the autocrine phosphorylation of STAT3 in isolated RA-FLS (Krause et al., 2002). Furthermore, RA-FLS are known to produce their own array of cytokines, such as IL-6, IL-15, IL-32 and IL-33 (Lefevre et al., 2015), found at higher levels in the synovial fluid of RA compared with OA patients (Altobelli et al., 2017; Hong et al., 2011; Kurowska et al., 2002; Matsuyama et al., 2012; Moon et al., 2012). Some of these cytokines might cooperatively contribute to maintaining enhanced STAT3 activity in an autocrine manner. Our gene expression analysis showed upregulation of IL-6, LIF and OSM expression in RA-FLS compared with OA-FLS grown in 3D-micromass. Signaling through these cytokines is inhibitable by JAK inhibitors; thus, we propose that simultaneous inhibition of these multiple cytokines possibly accounts for the superior effect of JAK inhibitors compared with specific cytokine blockade by anti-cytokine antibody. The gene expression analysis also revealed a potential contribution of several types of PDGF in hyperplastic behavior of RA-FLS, but we have not yet determined if blockade of PDGF occurs in our 3D-assay system. In addition to the enhancement of STAT3 phosphorylation, higher levels of total STAT3 protein were also observed in RA-FLS. This may be explained by the existence of hypo-methylated loci in the STAT3 gene in RA-FLS, which can increase STAT3 expression (Nakano et al., 2013).

One important finding in this study is that JAK inhibitors promoted RA-FLS cell death (Fig. 3). RA-FLS expressed higher levels of the anti-apoptotic genes, BCL2 and MCL1, compared with OA-FLS (Fig. 3B). This is consistent with a previous report showing that RA-FLS have higher levels of the BCL2 gene and are more resistant to soluble nitroprusside-induced apoptosis than OA-FLS (Lee et al., 2013), and provides the molecular basis underlying enhanced survival of RA-FLS. Given that these genes are regulated by STAT3 (Lee et al., 2013; Yue et al., 2015; Zhao et al., 2017) and JAK inhibitors suppressed the enhanced phosphorylation of STAT3 and accelerated RA-FLS cell death (Fig. 3A and C), it is likely that the cytokine milieu associated with RA potentiates the intrinsic pro-survival ability of RA-FLS and causes local accumulation of these cells, leading to synovial lining hyperplasia. Previous reports also indicate that extracellular stimuli such as IL-17 and IL-22 can decrease the rate of apoptosis in RA-FLS via the JAK-STAT3 pathway (Lee et al., 2013; Zhao et al., 2017). Considering the report showing that treatment of RA-FLS with JAK inhibitors itself does not induce apoptosis in RA-FLS (Diller et al., 2019), JAK inhibitors may work with environmental stress to accelerate apoptosis.

Using a 3D-micromass culture system, we found that JAK inhibitors attenuated self-directed formation of a hyperplastic lining-like structure by RA-FLS (Fig. 4). This provides direct evidence that JAK inhibitors can abrogate establishment of lining hyperplasia and development of pannus in RA. In this system, the thickness of lining by OA-FLS is reported to be 66.6% of that by RA-FLS. Our data show that the thickness by RA-FLS treated with peficitinib and tofacitinib was dose-related, and decreased up to 78.0% and 88.8% of DMSO control, respectively. Although we have not examined the effect of JAK inhibitors on the formation of lining-like structure by OA-FLS, these results may suggest that JAK inhibitors attenuate disease-related hyperplastic activity in RA-FLS and lining hyperplasia. The effect of JAK inhibition on lining hyperplasia was also proven in a rat arthritis model treated with tofacitinib (LaBranche et al., 2012), although the effect of peficitinib has yet to be determined. Previously, we and others reported that enhanced cell–cell and cell–extracellular matrix interactions mediated by cadherin-11 and integrin α9, respectively, play essential roles in the structural assembly of these structures (Emori et al., 2017; Kiener et al., 2006). However, JAK inhibitors did not alter cadherin-11 or integrin α9 protein levels in the 3D-culture system (Fig. 4). Also, JAK inhibitors do not affect adhesion of RA-FLS on plastic surface nor on endothelial cells

(Diller et al., 2019). JAK inhibitors might abrogate thickening of the synovium by promoting apoptosis, although we have yet to determine whether activation of STAT3 plays a crucial role in this process and whether there is enhanced apoptosis in 3D-cultured RA-FLS treated with JAK inhibitors. Notably, IL-6 receptor blockade (Fig. 4), like TNF-α blockade (Emori et al., 2017), did not disrupt the hyperplastic lining-like structure, emphasizing the unique action of JAK inhibitors in attenuating synovial hyperplasia. We also showed that JAK inhibition decreased spontaneous production of various pro-inflammatory mediators, including MMPs, IL-6, VEGF and TNFSF11 in 3D-cultured RA-FLS (Fig. 5A and C). This is consistent with a previous report that showed that ex vivo treatment of RA synovial explants with a JAK inhibitor decreases the production of pro-inflammatory mediators by altering mitochondrial function (McGarry et al., 2018), which may provide a mechanistic explanation for these effects. MMPs synthesized by RA-FLS cause damage to cartilage, whereas TNFSF11 expressed by RA-FLS mediates bone destruction by inducing osteoclastogenesis (Guo et al., 2018; Takayanagi et al., 2000). Upregulation of angiogenesis by VEGF is also prevalent in RA and is crucial for the development of pannus (Koch, 1998). Therefore, JAK inhibitors can ameliorate sustained synovitis and subsequent joint destruction by modulating the production of these pro-inflammatory mediators in RA-FLS.

Although the overall in vitro pharmacologic profile of peficitinib was comparable to that of tofacitinib (Table 1), peficitinib might be more advantageous for controlling joint inflammation than tofacitinib at a clinically relevant dose. In a phase 2 clinical trial for RA, peficitinib displayed a significant 50% improvement in the American College of Rheumatology criteria (ACR50) response at oral doses of 100 and 150 mg (Takeuchi et al., 2016). Based on the maximum plasma concentration (C_{max}) at 150 mg in healthy volunteers (613.2 ng/ml, Astellas Pharma, Inc.) and the protein-binding rate (72.83–75.20%, Astellas Pharma, Inc.), the unbound maximum plasma concentration ($C_{max,\ u}$) of peficitinib at this dose can be estimated as 466.0–510.4 nM (152.1–166.6 ng/ml), which seems sufficient to ameliorate the pathogenic activity of RA-FLS (Fig. 4A, D, 5A and 5C). In contrast, the estimated $C_{max,\ u}$ of tofacitinib at the approved dose (5 mg) is below 100 nM according to published information (Lamba et al., 2016; Pfizer Inc., 2012; Riese et al., 2010). Therefore, peficitinib may have higher efficacy against synovial inflammation than tofacitinib under clinical settings. In addition to the dosing advantage, peficitinib, but not tofacitinib, showed a trend towards decreasing STAT3 protein levels in RA-FLS (Figs. 3A and 4D). Consistent with this, peficitinib showed more potent induction of SNP-induced apoptosis (Fig. 3C) and more profound reduction in the formation of lining-like structure (Fig. 4A) and IL-6 and VEGF-A production by RA-FLS (Fig. 5A). Thus, increased STAT3 expression might be involved in these processes that are potentially more sensitive to peficitinib than tofacitinib. While findings from a panel of kinase assays (conducted by Carna Biosciences, Inc., Kobe, Japan; Supplementary Table 1) have yet to establish a unique mechanism for peficitinib, further investigation will be conducted to elucidate the mechanism for the differential effects.

4.1. Conclusions

Our data demonstrate that constitutive activation of the JAK-STAT pathway mediates the pro-inflammatory response and self-directed aggressive behavior of RA-FLS.

The novel JAK inhibitor, peficitinib, suppressed activation of STAT3, abrogated thickening of the synovium and inhibited production of pro-inflammatory mediators in RA-FLS. These multiple effects could not be achieved through inhibition of a single cytokine, which emphasizes the therapeutic value of JAK inhibitors in addressing persistent synovitis and progression of joint destruction in RA.

Funding

This study was funded by Astellas Pharma Inc. Editorial support was provided by Cello Health MedErgy (Europe) and funded by Astellas Pharma Inc.

Role of the funding source

The funder was responsible for the quality control of the data and the decision to submit an article for publication.

Authors' contributions

TE conducted the study, performed experiments and drafted the manuscript. MK performed experiments. SS, YH, SN and YF participated in the design and coordination of the study. HI and MH collected patient samples and provided critical comments on interpretation of the data. All authors read and approved the final manuscript for submission.

Ethics approval and consent to participate

Ethical approval for this study was granted by the Ethics Committee of Kyoto University Graduate School and the Faculty of Medicine and Astellas Research Ethics Committee. Informed consent was obtained from all patients prior to sample collection.

Availability of data and material

The datasets generated and analyzed in the current study are available from the corresponding author upon reasonable request. Peficitinib, tofacitinib and baricitinib used in this study will not be supplied based on the company policy of Astellas Pharma Inc.

Author agreement

We can confirm that this manuscript is original work, has not been published and is not under consideration for publication elsewhere. All authors had full access to the study data, satisfy the conditions for authorship as specified by the ICMJE criteria and approved the manuscript for submission. Funding sources, potential competing interests of the authors and the provision of medical writing support are detailed at the end of the manuscript in accordance with journal requirements.

CRediT authorship contribution statement

Takashi Emori: Investigation, Data curation, Writing - original draft, Writing - review & editing, Visualization, Supervision, Project administration. **Michiko Kasahara:** Investigation, Data curation, Writing - review & editing. **Shingo Sugahara:** Formal analysis, Methodology, Project administration, Writing - review & editing. **Motomu Hashimoto:** Supervision, Project administration, Writing - review & editing. **Hiromu Ito:** Supervision, Project administration, Writing - review & editing. **Shuh Narumiya:** Conceptualization, Methodology, Supervision, Project administration, Writing - review & editing. **Yasuyuki Higashi:** Supervision, Project administration, Writing - review & editing. **Yasutomo Fujii:** Supervision, Project administration, Writing - review & editing.

Declaration of competing interest

TE, MK, SS, YH and YF are employees of Astellas Pharma Inc. YH has a patent for peficitinib. SN is a scientific advisor to Astellas Pharma Inc. HI received a grant from Bristol-Myers Squibb Co., Ltd. and Asahi Kasei for other unrelated work. The Department of Advanced Medicine

for Rheumatic Diseases at the Graduate School of Medicine, Kyoto University, is supported by Nagahama City, Shiga, Japan and four pharmaceutical companies (Mitsubishi Tanabe Pharma Co., Chugai Pharmaceutical Co., Ltd, UCB Japan Co., Ltd, and AYUMI Pharmaceutical Co.). The KURAMA cohort study is supported by a grant from Daiichi Sankyo Co., Ltd. MH received research grant and/or speaker fees from Astellas Pharma Inc., Eisai Co., Ltd., Mitsubishi Tanabe Pharma Co., and Bristol-Myers Squibb Co., Ltd for other unrelated work.

Acknowledgements

We appreciate the critical reading by Satoshi Ushijima. Assistance in drafting the initial version of the manuscript was provided by Lisa O'Rourke, PhD, for Cello Health MedErgy (Europe). Editorial support was funded by Astellas Pharma Inc. We also thank Ritsuko Matsuda and Koichiro Torigoe for quality control of the presented data.

Appendix A. Supplementary data

Supplementary data to this article can be found online at https://doi.org/10.1016/j.ejphar.2020.173238.

References

Altman, R., Asch, E., Bloch, D., Bole, G., Borenstein, D., Brandt, K., Christy, W., Cooke, T.D., Greenwald, R., Hochberg, M., 1986. Development of criteria for the classification and reporting of osteoarthritis. Classification of osteoarthritis of the knee. Diagnostic and Therapeutic Criteria Committee of the American Rheumatism Association. Arthritis Rheum. 29, 1039–1049.

Altobelli, E., Angeletti, P.M., Piccolo, D., De Angelis, R., 2017. Synovial fluid and serum concentrations of inflammatory markers in rheumatoid arthritis, psoriatic arthritis and osteoarthritis: a systematic review. Curr. Rheumatol. Rev. 13, 170–179. https://doi.org/10.2174/1573397113666170427125918.

Arnett, F.C., Edworthy, S.M., Bloch, D.A., McShane, D.J., Fries, J.F., Cooper, N.S., Healey, L.A., Kaplan, S.R., Liang, M.H., Luthra, H.S., 1988. The American Rheumatism Association 1987 revised criteria for the classification of rheumatoid arthritis. Arthritis Rheum. 31, 315–324.

Banerjee, S., Biehl, A., Gadina, M., Hasni, S., Schwartz, D.M., 2017. JAK–STAT signaling as a target for inflammatory and autoimmune diseases: current and future prospects. Drugs 77, 521–546. https://doi.org/10.1007/s40265-017-0701-9.

Bartok, B., Firestein, G.S., 2010. Fibroblast-like synoviocytes: key effector cells in rheumatoid arthritis. Immunol. Rev. 233, 233–255. https://doi.org/10.1111/j.0105-2896.2009.00859.x.

Bottini, N., Firestein, G.S., 2013. Duality of fibroblast-like synoviocytes in RA: passive responders and imprinted aggressors. Nat. Rev. Rheumatol. 9, 24–33. https://doi.org/10.1038/nrrheum.2012.190.

Cho, M.-L., Cho, C.-S., Min, S.-Y., Kim, S.-H., Lee, S.-S., Kim, W.-U., Min, D.-J., Min, J.-K., Youn, J., Hwang, S.-Y., Park, S.-H., Kim, H.-Y., 2002. Cyclosporine inhibition of vascular endothelial growth factor production in rheumatoid synovial fibroblasts. Arthritis Rheum. 46, 1202–1209. https://doi.org/10.1002/art.10215.

Diller, M., Hasseli, R., Hülser, M.L., Aykara, I., Frommer, K., Rehart, S., Müller-Ladner, U., Neumann, E., 2019. Targeting activated synovial fibroblasts in rheumatoid arthritis by peficitinib. Front. Immunol. 10, 1–11. https://doi.org/10.3389/fimmu.2019.00541.

Emori, T., Hirose, J., Ise, K., Yomoda, J., Kasahara, M., Shinkuma, T., Yoshitomi, H., Ito, H., Hashimoto, M., Sugahara, S., Fujita, H., Yamamoto, N., Morita, Y., Narumiya, S., Aramori, I., 2017. Constitutive activation of integrin α9 augments self-directed hyperplastic and proinflammatory properties of fibroblast-like synoviocytes of rheumatoid arthritis. J. Immunol. 199, 3427–3436. https://doi.org/10.4049/jimmunol.1700941.

Gao, W., McCormick, J., Connolly, M., Balogh, E., Veale, D.J., Fearon, U., 2015. Hypoxia and STAT3 signalling interactions regulate pro-inflammatory pathways in rheumatoid arthritis. Ann. Rheum. Dis. 74, 1275–1283. https://doi.org/10.1136/annrheumdis-2013-204105.

Guo, Q., Wang, Y., Xu, D., Nossent, J., Pavlos, N.J., Xu, J., 2018. Rheumatoid arthritis: pathological mechanisms and modern pharmacologic therapies. Bone Res. 6, 15. https://doi.org/10.1038/s41413-018-0016-9.

Heinrich, P.C., Behrmann, I., Müller-Newen, G., Schaper, F., Graeve, L., 1998. Interleukin-6-type cytokine signalling through the gp130/Jak/STAT pathway. Biochem. J. 334 (Pt 2), 297–314.

Hong, Y.-S., Moon, S.-J., Joo, Y.-B., Jeon, C.-H., Cho, M.-L., Ju, J.H., Oh, H.-J., Heo, Y.-J., Park, S.-H., Kim, H.-Y., Min, J.-K., 2011. Measurement of interleukin-33 (IL-33) and IL-33 receptors (sST2 and ST2L) in patients with rheumatoid arthritis. J. Kor. Med. Sci. 26, 1132–1139. https://doi.org/10.3346/jkms.2011.26.9.1132.

Ikari, Y., Isozaki, T., Tsubokura, Y., Kasama, T., 2019. Peficitinib inhibits the chemotactic activity of monocytes via proinflammatory cytokine production in rheumatoid arthritis fibroblast-like synoviocytes. Cells 8, 561. https://doi.org/10.3390/cells8060561.

Ito, M., Yamazaki, S., Yamagami, K., Kuno, M., Morita, Y., Okuma, K., Nakamura, K., Chida, N., Inami, M., Inoue, T., Shirakami, S., Higashi, Y., 2017. A novel JAK inhibitor, peficitinib, demonstrates potent efficacy in a rat adjuvant-induced arthritis model. J. Pharmacol. Sci. 133, 25–33. https://doi.org/10.1016/j.jphs.2016.12.001.

Kiener, H.P., Lee, D.M., Agarwal, S.K., Brenner, M.B., 2006. Cadherin-11 induces rheumatoid arthritis fibroblast-like synoviocytes to form lining layers in vitro. Am. J. Pathol. 168, 1486–1499. https://doi.org/10.2353/ajpath.2006.050999.

Koch, A.E., 1998. Angiogenesis: implications for rheumatoid arthritis. Arthritis Rheum. 41, 951–962. https://doi.org/10.1002/1529-0131(199806)41:6<951::AID-ART2>3.0.CO;2-D.

Krause, A., Scaletta, N., Ji, J.-D., Ivashkiv, L.B., 2002. Rheumatoid arthritis synoviocyte survival is dependent on Stat3. J. Immunol. 169, 6610–6616. https://doi.org/10.4049/jimmunol.169.11.6610.

Kurowska, M., Rudnicka, W., Kontny, E., Janicka, I., Chorazy, M., Kowalczewski, J., Ziółkowska, M., Ferrari-Lacraz, S., Strom, T.B., Maśliński, W., 2002. Fibroblast-like synoviocytes from rheumatoid arthritis patients express functional IL-15 receptor complex: endogenous IL-15 in autocrine fashion enhances cell proliferation and expression of Bcl-x(L) and Bcl-2. J. Immunol. 169, 1760–1767. https://doi.org/10.4049/jimmunol.169.4.1760.

LaBranche, T.P., Jesson, M.I., Radi, Z.A., Storer, C.E., Guzova, J.A., Bonar, S.L., Thompson, J.M., Happa, F.A., Stewart, Z.S., Zhan, Y., Bollinger, C.S., Bansal, P.N., Wellen, J.W., Wilkie, D.P., Bailey, S.A., Symanowicz, P.T., Hegen, M., Head, R.D., Kishore, N., Mbalaviele, G., Meyer, D.M., 2012. JAK inhibition with tofacitinib suppresses arthritic joint structural damage through decreased RANKL production. Arthritis Rheum. 64, 3531–3542. https://doi.org/10.1002/art.34649.

Lamba, M., Wang, R., Fletcher, T., Alvey, C., Kushner, J., Stock, T.C., 2016. Extended-release once-daily formulation of tofacitinib: evaluation of pharmacokinetics compared with immediate-release tofacitinib and impact of food. J. Clin. Pharmacol. 56, 1362–1371. https://doi.org/10.1002/jcph.734.

Lee, S.-Y., Kwok, S.-K., Son, H.-J., Ryu, J.-G., Kim, E.-K., Oh, H.-J., Cho, M.-L., Ju, J., Park, S.-H., Kim, H.-Y., 2013. IL-17-mediated Bcl-2 expression regulates survival of fibroblast-like synoviocytes in rheumatoid arthritis through STAT3 activation. Arthritis Res. Ther. 15, R31. https://doi.org/10.1186/ar4179.

Lefevre, S., Meier, F.M.P., Neumann, E., Muller-Ladner, U., 2015. Role of synovial fibroblasts in rheumatoid arthritis. Curr. Pharmaceut. Des. 21, 130–141.

Matsuyama, Y., Okazaki, H., Hoshino, M., Onishi, S., Kamata, Y., Nagatani, K., Nagashima, T., Iwamoto, M., Yoshio, T., Ohto-Ozaki, H., Tamemoto, H., Komine, M., Sekiya, H., Tominaga, S., Minota, S., 2012. Sustained elevation of interleukin-33 in sera and synovial fluids from patients with rheumatoid arthritis non-responsive to anti-tumor necrosis factor: possible association with persistent IL-1β signaling and a poor clinical response. Rheumatol. Int. 32, 1397–1401. https://doi.org/10.1007/s00296-011-1854-6.

McGarry, T., Orr, C., Wade, S., Biniecka, M., Wade, S., Gallagher, L., Low, C., Veale, D.J., Fearon, U., 2018. JAK/STAT blockade alters synovial bioenergetics, mitochondrial function, and proinflammatory mediators in rheumatoid arthritis. Arthritis Rheum. 70, 1959–1970. https://doi.org/10.1002/art.40569.

Moon, Y.-M., Yoon, B.-Y., Her, Y.-M., Oh, H.-J., Lee, J.-S., Kim, K.-W., Lee, S.-Y., Woo, Y.-J., Park, K.-S., Park, S.-H., Kim, H.-Y., Cho, M.-L., 2012. IL-32 and IL-17 interact and have the potential to aggravate osteoclastogenesis in rheumatoid arthritis. Arthritis Res. Ther. 14, R246. https://doi.org/10.1186/ar4089.

Nakano, K., Whitaker, J.W., Boyle, D.L., Wang, W., Firestein, G.S., 2013. DNA methylome signature in rheumatoid arthritis. Ann. Rheum. Dis. 72, 110–117. https://doi.org/10.1136/annrheumdis-2012-201526.

Nakayamada, S., Kubo, S., Iwata, S., Tanaka, Y., 2016. Recent progress in JAK inhibitors for the treatment of rheumatoid arthritis. BioDrugs 30, 407–419. https://doi.org/10.1007/s40259-016-0190-5.

Pfizer Inc., 2012. Xeljanz® (tofacitinib) prescribing information. URL. https://www.accessdata.fda.gov/drugsatfda_docs/label/2018/203214s018lbl.pdf, Accessed date: 8 April 2020.

Riese, R.J., Krishnaswami, S., Kremer, J., 2010. Inhibition of JAK kinases in patients with rheumatoid arthritis: scientific rationale and clinical outcomes. Best Pract. Res. Clin. Rheumatol. 24, 513–526. https://doi.org/10.1016/j.berh.2010.02.003.

Takayanagi, H., Iizuka, H., Juji, T., Nakagawa, T., Yamamoto, A., Miyazaki, T., Koshihara, Y., Oda, H., Nakamura, K., Tanaka, S., 2000. Involvement of receptor activator of nuclear factor κB ligand/osteoclast differentiation factor in osteoclastogenesis from synoviocytes in rheumatoid arthritis. Arthritis Rheum. 43, 259. https://doi.org/10.1002/1529-0131(200002)43:2<259::AID-ANR4>3.0.CO;2-W.

Takeuchi, T., Tanaka, Y., Iwasaki, M., Ishikura, H., Saeki, S., Kaneko, Y., 2016. Efficacy and safety of the oral Janus kinase inhibitor peficitinib (ASP015K) monotherapy in patients with moderate to severe rheumatoid arthritis in Japan: a 12-week, randomised, double-blind, placebo-controlled phase IIb study. Ann. Rheum. Dis. 75, 1057–1064. https://doi.org/10.1136/annrheumdis-2015-208279.

Wang, D., Li, Y., Liu, Y., Shi, G., 2014. The use of biologic therapies in the treatment of rheumatoid arthritis. Curr. Pharmaceut. Biotechnol. 15, 542–548.

Xie, K., Wang, Y., Huang, S., Xu, L., Bielenberg, D., Salas, T., McConkey, D.J., Jiang, W., Fidler, I.J., 1997. Nitric oxide-mediated apoptosis of K-1735 melanoma cells is associated with downregulation of Bcl-2. Oncogene 15, 771–779. https://doi.org/10.1038/sj.onc.1201239.

Yue, W., Zheng, X., Lin, Y., Yang, C.S., Xu, Q., Carpizo, D., Huang, H., DiPaola, R.S., Tan, X.-L., 2015. Metformin combined with aspirin significantly inhibit pancreatic cancer cell growth *in vitro* and *in vivo* by suppressing anti-apoptotic proteins Mcl-1 and Bcl-2. Oncotarget 6, 21208–21224. https://doi.org/10.18632/oncotarget.4126.

Zhao, M., Li, Y., Xiao, W., 2017. Anti-apoptotic effect of interleukin-22 on fibroblast-like synoviocytes in patients with rheumatoid arthritis is mediated via the signal transducer and activator of transcription 3 signaling pathway. Int. J. Rheum. Dis. 20, 214–224. https://doi.org/10.1111/1756-185X.12939.